*Quantum Electronics* **48** (4) 344–350 (2018) 

https://doi.org/10.1070/QEL16677

# Formation of nanosecond SBS-compressed pulses for pumping an ultra-high power parametric amplifier

A.A. Kuz'min, O.V. Kulagin, V.I. Rodchenkov

*Abstract.* **Compression of pulsed Nd:glass laser radiation under stimulated Brillouin scattering (SBS) in perfluorooctane is investigated. Compression of 16-ns pulses at a beam diameter of 30 mm is implemented. The maximum compression coefficient is 28 in the optimal range of laser pulse energies from 2 to 4 J. The Stokes pulse power exceeds that of the initial laser pulse by a factor of about 11.5. The Stokes pulse jitter (fluctuations of the Stokes pulse exit time from the compressor) is studied. The rms spread of these fluctuations is found to be 0.85 ns.**

***Keywords:*** *Nd:glass laser, SBS pulse compression, pumping for an ultra-high power parametric amplifier, Stokes pulse jitter.*

## 1. Introduction

The concept of pulse compression at the laser system output due to the stimulated light scattering has been actively developed since the end of the 1970s [1–4]. These experiments were inspired by the studies in the field of laser fusion, where a very important task is to increase the light intensity on a target.

The most promising methods for shortening laser pulses with an energy of several hundred joules or higher are compression under conditions of stimulated Brillouin scattering (SBS) [5] and compression under stimulated Raman scattering (SRS) [6]. SRS is characterised by a significant frequency shift, which ranges approximately from 500 to 1100 $cm^{-1}$ for different media; in the case of SBS, it is 0.1 $cm^{-1}$, a value less than 0.0001 of the frequency of visible or IR light. This frequency shift is smaller than the gain band for practically all laser media, due to which a converted laser pulse can be amplified in the same medium as the initial one. Therefore, nonlinear media are used as materials for SBS mirrors in multipass laser amplifiers [7]. At the same time, the effect of competing types of scattering on SBS is most insignificant.

SBS compression has been successfully applied for a rather long time in systems with a pulse energy up to several joules [5] and still remains important [8]. Nevertheless, the number of studies devoted to the SBS compression of pulses with energies of several hundred joules is very small. Little attention has been paid to practical aspects of this problem. From the end of the 1990s to the beginning of the 2000s, the possibility of compressing pulsed Nd:glass laser radiation with an energy of several hundred joules was experimentally studied at the Research Institute for Complex Testing of Optoelectronic Devices and Systems (Sosnovyi Bor, Leningrad region, Russia) [9, 10]. The possibility of energy scaling of Nd:glass laser–SBS compressor systems to a pump energy of 750 J was demonstrated. The initial 70-ns pulse was compressed to 2–4 ns with an energy conversion efficiency into short pulse of 60%. However, these studies have not received further practical development.

Currently, the interest in SBS compression of high-energy pulses remains high in view of the development of laser fusion projects. In particular, the LIFE project implies coherent combining of 25 channels (100 J in each) due to the use of phase conjugation under SBS [11]. However, as previously, little attention is paid to SBS compression of high-energy pulses. Until now, the method of SBS pulse compression have been undeservedly rejected when designing and elaborating ultra-high power laser systems, which undoubtedly have their own specificity. In addition, some physical aspects of SBS (previously disregarded) become important for these systems; correspondingly, they should be studied in detail.

Subpetawatt and petawatt lasers [12] are generally attributed to ultra-high power laser systems. There are projects of multipetawatt systems. The operation of these systems is based on the chirped pulse amplification (CPA) method [13]. Arbitrarily, ultra-high power lasers can be separated into three types. CPA is implemented in neodymium glass [14], Ti:sapphire crystals [15], and parametric DKDP crystals [16] in the lasers of the first, second, and third types, respectively. Optical parametric chirped pulse amplification (OPCPA) occurs in the latter. Based on this technology, we developed a 0.56-PW laser complex PEARL at our laboratory in 2007 [16], the world's first parametric system of petawatt level.

The second harmonic of Nd:glass laser radiation is used to pump either Ti:sapphire crystals or parametric DKDP crystals in the systems of the second and third types. The advantages and drawbacks of the three aforementioned approaches to obtaining multipetawatt power were analysed in [17]. The main drawback of the systems based on Nd:glass is the narrow gain band, which limits the compressed pulse width to a level of several hundred femtoseconds; hence, an advance to the multipetawatt range calls for pulses with energies on the order of several kilojoules. However, optically resistant diffraction gratings capable of compressing such pulses have not been developed yet. Ti:sapphire systems and DKDP-based parametric amplifiers provide broadband amplification, which makes it possible to compress pulses to about 20 fs; i.e., the energy necessary to obtain the same peak power in Nd:glass systems is several tens of times lower.

**A.A. Kuz'min, O.V. Kulagin, V.I. Rodchenkov** Institute of Applied Physics, Russian Academy of Sciences, ul. Ul'yanova 46, 603950 Nizhny Novgorod, Russia; e-mail: alexeyhsgap@yandex.ru, ok@appl.sci-nnov.ru, rvi47@mail.ru

Received 14 March 2018
*Kvantovaya Elektronika* **48** (4) 344–350 (2018)
Translated by Yu.P. Sin'kov

The existing technologies make it possible to grow Ti : sapphire crystals with an aperture of about 20 cm. The sizes of manufactured DKDP crystals are twice as large. The OPCPA principle has a number of advantages over CPA: (i) very high gain per pass (10000 in comparison with 10 in the case of CPA); (ii) absence of self-excitation and amplified spontaneous luminescence; (iii) high temporal contrast of the compressed pulse in view of the nonlinear character of amplification; (iv) absence of heat release in the parametric crystal, related to the quantum defect; and (v) smaller (than in the CPA scheme) spectral distortion, because the gain saturation, caused by population inversion depletion, is absent in this case. Due to these advantages, we believe the principle of parametric amplification of pulses to be most promising for advancing to the multipetawatt power range. At the same time, a significant drawback of OPCPA is that one must use a short (~1 ns) pump pulse, because a parametric amplifier, in contrast to a laser one, cannot accumulate energy in the form of population inversion, and the pump pulse width should be comparable with that of a stretched femtosecond pulse. The requirements to synchronisation of chirped and pump pulses are stringent for the same reason. Here, the time jitter (uncontrolled random deviation of one pulse in time with respect to the other pulse) should not exceed ~0.1 ns.

Thus, all OPCPA advantages are related directly to the amplifier, while the drawbacks are determined by the pump laser, which must satisfy more stringent requirements than in the case of CPA. At a pump pulse width of ~1 ns, the breakdown threshold of optical elements is much lower than for pulses several tens of nanoseconds long [18], as, e.g., in lasers for pumping Ti : sapphire. An enormous problem is beam self-focusing. When long (several tens of nanoseconds) pulses are used, these limitations are much less stringent.

To overcome the limitations caused by the short width of pump pulses in the OPCPA scheme, we propose to use the technique of SBS pulse compression. Within this approach, a pump laser for a parametric crystal, as in the case where Ti : sapphire is pumped, will generate long (several tens of nanoseconds) pulses. This will make it possible to reduce the limitations imposed by the optical breakdown of elements, beam self-focusing, and pulse profile distortions, as well as to increase the amplifier output energy. Then the long-pulse energy can be transferred (by means of SBS) to a short nanosecond pulse with a Stokes frequency shift in order to pump a parametric crystal.

To satisfy the stringent requirements to synchronisation of the pump and chirped femtosecond pulses in the OPCPA scheme, one should study the Stokes pulse jitter, which is related to the fluctuation nature of SBS seeding. This issue has not been investigated previously, because it is not necessary to synchronise laser pulses from different sources in conventional applications of SBS compression. It is assumed that in the conventional (the simplest) scheme of an SBS compressor, where an initial pulse is focused in a long cell (the light travel time from the cell input to the focal waist should exceed half of the compressed pulse width), the Stokes pulse jitter should be on the order of the light travel time through the focal waist. This time generally does not exceed several picoseconds, which is much less than the acceptable error in synchronising pulses in the OPCPA scheme. This situation is typical of most practical cases, where pulses are compressed under conditions of strongly time-dependent SBS. Another situation may occur in the case we are interested in: compression of pulses that are long on the scale of the hypersound relaxation time in a nonlinear medium. This time scale may be decisive for the Stokes pulse jitter. It is intuitively clear that the hypersound decay time should be as short as possible to reduce jitter.

Among the most appropriate media for SBS compression of high-energy pulses, which are characterised by the shortest hypersound relaxation time (less than 1 ns), we should select liquid Freons, in particular, fluorocarbons (perfluorinated hydrocarbons) [19]. In this paper, we report the results of studying the SBS compression of 16-ns Nd : glass laser pulses in perfluorooctane ($C_8F_{18}$). The emphasis is on measuring the Stokes pulse jitter in the single-cell compression scheme.

## 2. Experimental setup

To perform experiments on pulse compression, we developed a system, whose schematic is shown in Fig. 1a. The light source was the pump laser of the PEARL complex, operating in the regime of giant pulse amplification. The pulses had a shape close to Gaussian with a duration $\Delta t_{las}$ equal to 16 ns (FWHM). The setup included also an SBS compressor (a cell 3 m long and 35 mm in diameter, filled with perfluorooctane; Fig. 1b); a polariser and a quarter-wave plate for optical beam decoupling at the input and output of the compressor; a lens to focus the laser beam into the cell; and diagnostic systems for laser and Stokes pulses, including glass wedges, SDU285R digital cameras with Sony CCD ICX285AL sensors for measuring beam intensity distributions, Gentec-EO QE50LP-S-MB-D0 pulse energy meters, and Thorlabs SIR5-FC photodiodes with a time response less than 0.1 ns for measuring the pulse shape. Signals from photodiodes were recorded using a Tektronix DPO71254C oscilloscope with a transmission band of 12.5 GHz. The laser-beam diameter on the cell input window was 30 mm, and the focal waist was located at a distance of $z_f = 2635$ mm from this window. The condition necessary for implementing SBS compression, $z_f > c\Delta t_{las}/(2n)$ ($c$ is the speed of light in vacuum and $n = 1.268$ is the refractive index of perfluorooctane at the wavelength $\lambda = 1054$ nm), was satisfied.

The physical properties of perfluorooctane, which characterise the SBS occurring in it, were investigated in detail in [19, 20]. In particular, the following values were found: room-temperature density $\rho_0 = 1.77$ g cm$^{-3}$, hypersound decay time (by a factor of e) $\tau_R = 0.8-0.9$ ns, hypersound velocity $v_s = 563$ m s$^{-1}$, and steady-state Stokes wave gain (under SBS conditions) 4.7 cm GW$^{-1}$. Advantages of these media (including perfluorooctane) are, in particular, relatively high thresholds for optical breakdown and other nonlinear optical effects (SRS, self-focusing) and low absorption in the visible and near-IR ranges [21]. To implement efficiently these advantages, it is necessary to purify SBS media from both disperse and dissolved molecular impurities.

The perfluorooctane used in our experiments was highly purified by fluid rectification in a packed column. In this rectification method, the contact surface of countercurrent liquid and vapour phases is formed in a vertical column-type apparatus with a dispersive solid head under three-phase fluidised bed conditions [22, 23].

This method is highly efficient for deep purification of halogen-containing liquids from impurities in the molecularly dissolved form due to the well-developed phase contact surface. In addition, this method is efficient for purification from microdisperse impurities, because convective diffusion of submicron suspended particles in vapour to the absorbing interface [24, 25] occurs during rectification.

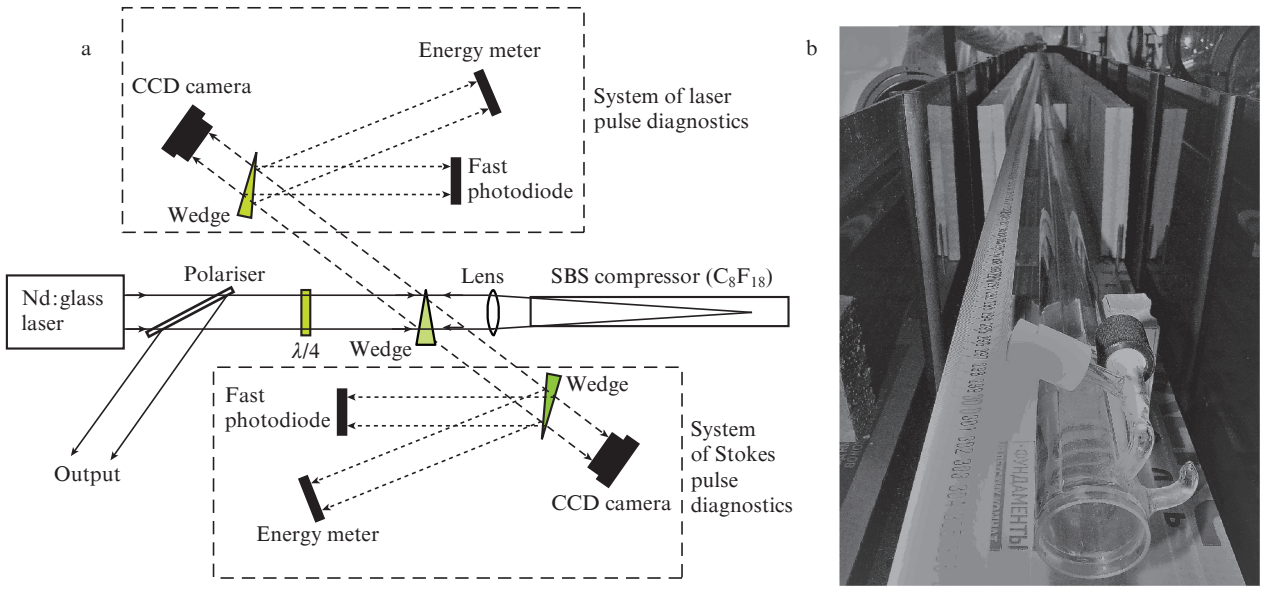


**Figure 1.** (a) Schematic of the experimental setup and (b) a photograph of the SBS compressor.

Special attention was paid to the conservation of perfluorooctane purity when filling the SBS cell. To exclude microdisperse phase background, the cell inner surface was processed (using a specially developed technique) by a strong agent: oxidant prepared based on concentrated hydrogen peroxide. Before filling, the SBS cell was washed for a long time by a high-purity perfluorooctane flow directly from the rectification column.

All stages of nonlinear-medium purification and cell fabrication were carried out at the Institute of Applied Physics, Russian Academy of Sciences, using an original equipment developed by us. The concentration of absorbing submicron particles in the nonlinear liquid was decreased to no more than 1 $cm^{-3}$, and the content of hydrogen-containing impurities was diminished to less than $10^{-5}$ wt %. The SBS cell was placed in a heat-insulating box in order to reduce the temperature gradients in the nonlinear medium and exclude the beam refraction along the cell.

## 3. Experimental results

The laser pulse energy in the experiments was varied in the range of 0–8.5 J. The laser beam had a super-Gaussian intensity distribution (Figs 2a, 2c), and its divergence exceeded the diffraction divergence by a factor of 2.4; this circumstance determined an increase in the SBS threshold: the laser pulse energy at which 5% energy is scattered into the Stokes wave. Dependences of the Stokes pulse energy $E_s$ and reflectance $R_s$ on the laser pulse energy $E_{las}$ are shown in Fig. 3. It follows from these curves that the SBS threshold $E_{th}$ in our experiments amounted to 17.5 mJ, a value exceeding the threshold for radiation of diffraction quality by a factor of 5.8 [19]. An increase in energy led to a rapid rise in the reflectance, with saturation at a level of about 95% at energies higher than 1 J. The experimental dependence $R_s(E_{las})$ in Fig. 3 is close to the universal dependence from [26], described by the formula $R_s = 1/(1 + \alpha E_0/E_{las})$, where $E_{las} > E_0$; $E_0$ is some constant energy characterising the nonlinear medium (in our case, $E_0 = 9.5$ mJ); and $\alpha = 6$ is the universal coefficient for time-dependent SBS. The agreement between the experimental and theoretical dependences $R_s(E_{las})$ indicates the absence of minor nonlinear effects competing with SBS.

Figure 4 presents the dependence of the Stokes pulse FWHM $\Delta t_s$ on the laser pulse energy. It was about 5 ns at the SBS threshold. The Stokes pulse width decreased with increasing laser pulse energy. The largest compression coefficient (27.7) was attained in the energy range of 2–4 J. The minimum measured $\Delta t_s$ value turned out to be 0.56 ns. Oscillograms of laser and Stokes pulses at different energies $E_{las}$ are shown in Fig. 5. These oscillograms present aperture-averaged pulse powers; when recording them, matte plates were installed before fast photodiodes to mix rays from different points of beam cross sections. While the laser pulse energy increased and optimal compression was reached at $E_{las} = 3.5$ J (Fig. 5c), an oscillating tail arose (behind the main Stokes peak), which contained about 50% Stokes energy. The presence of a tail indicates that the chosen cell length was not optimal for complete energy transfer to the main peak. The main Stokes pulse leaves the nonlinear medium before the laser pulse enters it entirely. This tail can be eliminated by choosing a longer cell. At the same time, the maximum degree of laser pulse compression that was observed in our experiments is close to the ultimate attainable one [27].

The degree of compression decreased at laser pulse energies of 4 J and higher. The increasing effect of focal waist screening by the bulk hypersonic grating led to a decrease in the interaction length of laser and Stokes pulses. The effective scattering region shifted to the input cell window. As a result, along with an increase in the width of the main Stokes pulse, the tail also grew; at an energy of about 8 J, the tail had a shape close to that of the incident laser pulse and contained almost all scattered energy (Fig. 5d).

The time scale in Fig. 5 is referenced to the laser pulse. The zero instant is taken to be the position of the laser pulse centre, estimated from the area under the oscillogram. If the laser pulse energy was entirely transferred to the Stokes pulse at the focal point, the Stokes pulse oscillogram would repeat the laser pulse shape and be centred at zero point. Since the main Stokes peak arises specifically in the focal waist in the SBS cell, its position ($t_s$) in the oscillograms determines the part of

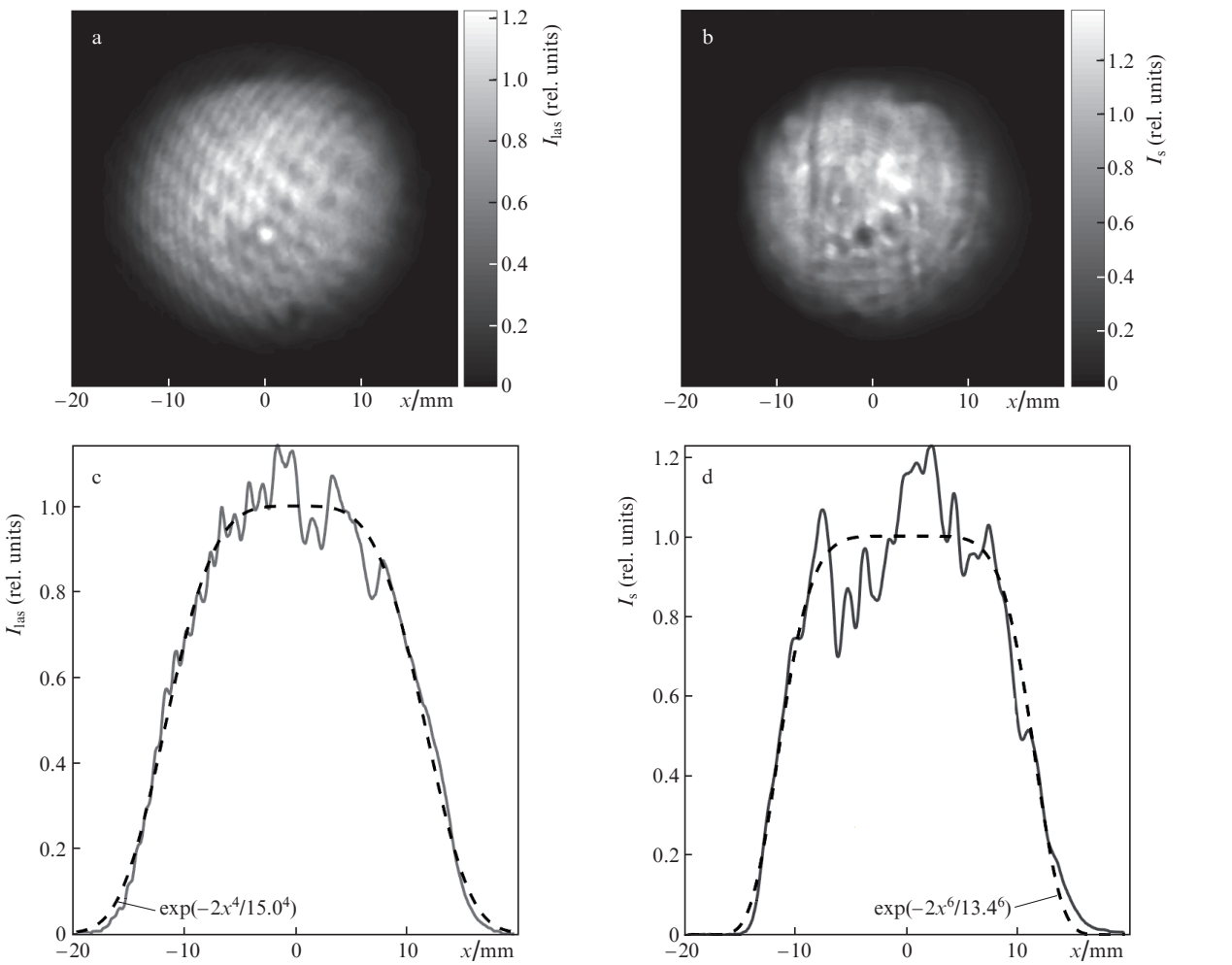


**Figure 2.** Normalised intensity distributions in the (a) laser ($I_{las}$) and (b) Stokes ($I_s$) beams and (c, d) their cross sections along the transverse coordinate ($y = 0$) (solid lines; the dashed lines are approximations of the experimental profiles, described by the formulas given in the lower panels).

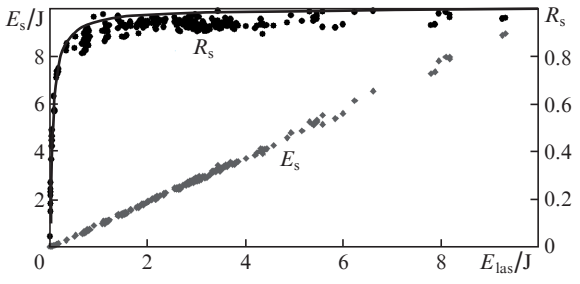


**Figure 3.** Dependences of the energy $E_s$ and reflectance $R_s$ of a Stokes pulse on the laser pulse energy $E_{las}$ (symbols are experimental data, and the solid line is the dependence $R_s(E_{las})$ from [26], which is universal for SBS).

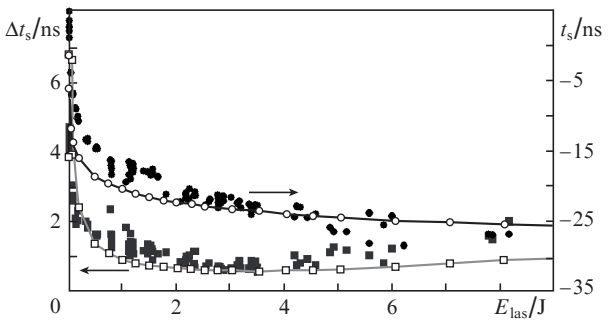


**Figure 4.** Experimental (filled symbols) and theoretical (open symbols) dependences of the Stokes pulse width and peak position (in the laser pulse frame of reference) on the laser pulse energy.

the initial laser pulse from which this peak is formed. For example, at the SBS threshold, the Stokes pulse is formed in the focal waist when the laser pulse maximum reaches it; therefore, the Stokes peak is located at zero point on the time scale ($t_s = 0$) in Fig. 5a. The oscillations in the Stokes pulse tail do not arise in the focal waist; they are due to the laser pulse scattering from the hypersonic grating formed throughout the entire volume of nonlinear medium. Therefore, their position with respect to the laser pulse in the above oscillograms does not characterise the part of the pulse they are formed from. For example, the second peak of the Stokes pulse in Fig. 5d in the vicinity of instant $t = -20$ ns corresponds to the reflection of laser pulse maximum. The range of 20 ns determines the reflection point for the latter. It is spaced from the focal waist towards the cell input at the distance passed by light in a nonlinear medium for 10 ns, i.e., is located near the SBS cell input window.

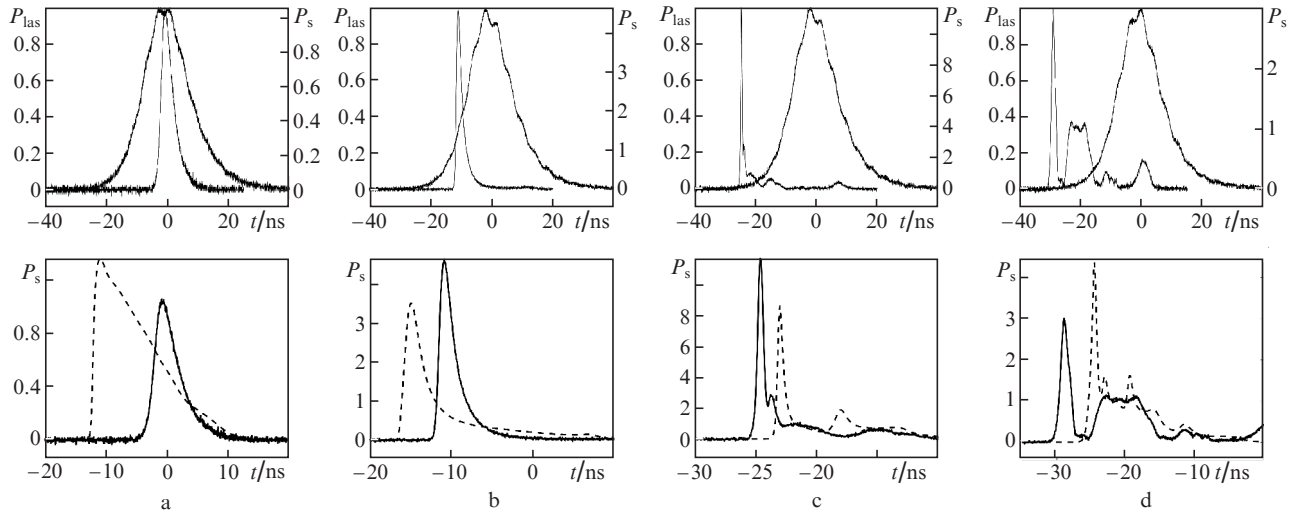


**Figure 5.** Oscillograms of laser ($P_{las}$) and Stokes ($P_s$) pulse powers, normalised to the laser pulse peak power, at different pulse energies and widths $\Delta t_{las}$ and $\Delta t_s$:
(a) $E_{las}$ = 30 mJ, $E_s$ = 8 mJ, $\Delta t_{las}$ = 16.97 ns, and $\Delta t_s$ = 4.23 ns; (b) $E_{las}$ = 160 mJ, $E_s$ = 110 mJ, $\Delta t_{las}$ = 15.61 ns, and $\Delta t_s$ = 2.00 ns; (c) $E_{las}$ = 3.5 J, $E_s$ = 3.3 J, $\Delta t_{las}$ = 15.52 ns, and $\Delta t_s$ = 0.56 ns; and (d) $E_{las}$ = 7.9 J, $E_s$ = 7.3 J, $\Delta t_{las}$ = 15.86 ns, and $\Delta t_s$ = 1.50 ns. Upper row: experimental oscillograms of laser and Stokes pulses. Lower row: experimental and theoretical (dashed lines) oscillograms of Stokes pulse.

We paid much attention to measuring the Stokes pulse jitter, which is a random deviation (from some average value) of the Stokes pulse escape time from the cell at identical laser pulse parameters. These time fluctuations are caused by the noise nature of SBS onset; their magnitude can be estimated from the spread of experimental $t_s$ points in Fig. 4 at a fixed laser pulse energy $E_{las}$. For clarity, Fig. 6a shows three superimposed oscillograms, obtained under conditions of optimal laser pulse compression. In all three cases the measured laser pulse energy was 3.4–3.5 J and the FWHM was $\Delta t_{las} = 15.8 \pm 0.1$ ns. The laser pulse oscillograms coincided with high accuracy, whereas the peaks of Stokes pulses deviated within 0.87 ns. Specifically this average spread of $t_s$ fluctuations was observed in all our experiments.

The fluctuations of the parameter $t_s$ were also measured by an alternative method. In the existing scheme of the PEARL pump laser, pulses with a width of about 1 ns (cut from giant pulses, as in our experiments on SBS compression, using a Pockels cell) are applied at the input of Nd:glass amplifiers. Part of the giant pulse remaining after cutting has a hole (see Fig. 6b). The Pockels cell response is synchronised with a femtosecond oscillator, so that a chirped femtosecond pulse and pump laser pulse (at doubled frequency) are intersected in a parametric DKDP crystal with an accuracy higher than 0.1 ns. Of practical interest is the synchronisation of the Stokes pulses obtained in our experiments with the pulses from femtosecond master oscillator or with the Pockels cell, which is the same in view of the aforesaid.

We performed an experiment on compression of a giant pulse with a hole in the trailing edge, cut by a Pockels cell. The cutting instant was intentionally shifted from the laser pulse peak to the tail in order to exclude the hole influence on the formation of the main Stokes peak. At identical laser pulse parameters, we measured the shift of the Stokes pulse peak with respect to the hole ($t_{peak\text{-}cut}$), which played the role of a time mark (Fig. 6b).

Based on the experimental results, we found the distribution function for the Stokes pulse jitter, $F(\delta t_s)$, which is graphically presented in Fig. 7. The step line is plotted according to

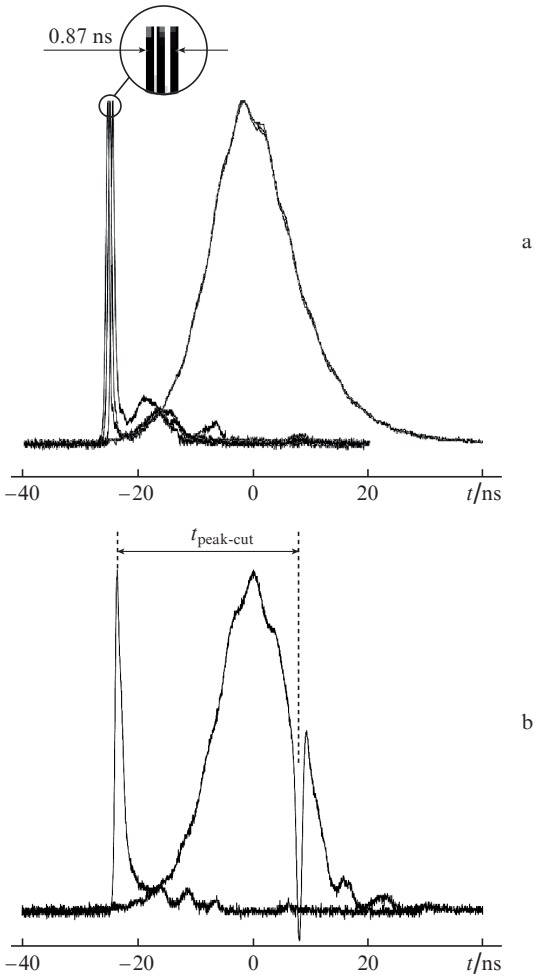


**Figure 6.** (a) Time fluctuations of the Stokes pulse peak position under SBS compression (three superimposed oscillograms; the laser pulses coincide, whereas the Stokes pulses diverge) and (b) a way of measuring jitter using a reference 'cut' in the laser pulse.

the experimental results, and the smooth line is an approximation of experimental data by normal distribution. The distribution function argument, $\delta t_s$, is the fluctuations of the $t_{\text{peak-cut}}$ value. By definition, function $F(\delta t_s)$ is the probability of the following event: the deviation of $t_{\text{peak-cut}}$ from its mean in a specific experimental realisation is equal to $\delta t_s$ or smaller. An analysis of the plotted distribution function suggests that the rms spread of random variable $\delta t_s$ is 0.85 ns. This value coincides with the spread of experimental points for parameter $t_s$ in Fig. 4. The experimental distribution function for Stokes pulse jitter coincides well with the normal distribution function having a parameter $\sigma$ (rms deviation) also equal to 0.85 ns.

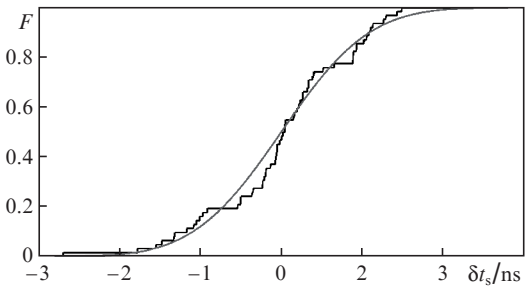


**Figure 7.** Distribution function for the Stokes pulse jitter: the step line is plotted based on experimental data and the smooth line is an approximation by a normal distribution with an rms deviation $\sigma = 0.85$ ns.

Proceeding from the experimental data obtained, we can conclude that the Stokes pulse jitter in the case of SBS compression of pulses that are long on the scale of the hypersound relaxation time is comparable with this characteristic time. Hence, the simple scheme of single-cell SBS compressor cannot be used to compress pump pulses in an ultra-high power parametric laser complex (such as PEARL) to a width of ~1 ns. However, the concept of SBS pulse compression is undoubtedly highly promising for developing multipetawatt parametric laser systems. The Stokes pulse time jitter can be reduced using the two-cell SBS amplifier/oscillator scheme. One can obtain a short Stokes pulse with a jitter less than 0.1 ns, moving towards a long high-energy laser pulse in the SBS amplifier cell, by cutting (using a Pockels cell, with a time stability better than 0.1 ns [16]) from a long low-energy Stokes pulse formed in the SBS oscillator cell (it is planned to design such a system in the nearest future). There are ways to reduce jitter in the single-cell scheme using a conventional mirror behind the SBS cell, which partially reflects backward the radiation passed behind the focal waist and provides Stokes pulse seeding. The application of this technique in [8] made it possible to reduce the Stokes pulse jitter by a factor of 3 at a laser pulse width of ~0.9 ns. However, the efficiency of this method for compressing pulses ~16 ns long remains disputable. Separate studies should be performed in this context; they are also planned in the nearest future.

To conclude, we should say some words about the design of SBS compressors. Among many mathematical models developed to describe SBS in focused beams, the model reported in [28] most completely takes into account the specific features of beam focusing and diffraction, as well as the influence of competing effects. This model is based on solving numerically the truncated nonlinear interaction equations for the laser, Stokes, and hypersonic waves. The aforementioned equations contain derivatives with respect to time and longitudinal coordinate and a Laplacian with respect to transverse coordinates. The model is not bound to the laser-beam shape at the input of the nonlinear medium. The computational resources of modern personal computers make it possible to apply easily this model to calculate SBS for real experimental beams, specifically this was done in our study. There is a certain difficulty with simulating the phase distortions in real laser beams. However, as our calculations showed, when the laser pulse energy exceeds several times the SBS threshold, the calculated Stokes pulse parameters (obtained on the assumption of a planar laser beam phase front before focusing into the cell) are close to the experimental results for a beam with a divergence exceeding the diffraction divergence by a factor of 2.4. Figures 4 and 5 show good agreement between the experimental and calculated data in the range of optimal (for compression) laser energies. Hence, the model proposed in [28] can be used to design different SBS compression schemes for the laser under consideration.

## 4. Conclusions

We developed an experimental bench for implementing SBS compression of 16-ns laser pulses in high-purity perfluorooctane. The SBS cell length and diameter were, respectively, 3 m and 35 mm. The optimal range of laser pulse energies, providing the highest degree of compression (by a factor of 27.7) and best efficiency of energy transfer to a short Stokes pulse (about 50%), was determined. At a laser pulse FWHM = 16 ns, the minimum Stokes pulse width turned out to be 0.56 ns. The Stokes pulse peak power exceeded the laser pulse power by a factor of about 11.5.

The rms spread of the Stokes pulse exit time from the cell, which is determined by the noise nature of SBS, was found to be 0.85 ns, a value close to the hypersound relaxation time in nonlinear media (0.8–0.9 ns). This fluctuation level is unacceptable when Stokes pulses are used to pump parametric amplifiers of chirped pulses in the PEARL laser complex and similar systems. Here, more complex schemes of an SBS compressor should be developed. We are planning to continue the work in this field.

***Acknowledgements.*** This work was performed within the Programme of Development of the Institute of Applied Physics, Russian Academy of Sciences, for 2016–2020 (Agreement No. 007-021225/2) and supported by the Presidium of the Russian Academy of Sciences (Programme 'Extreme Light Fields and Their Interaction with Matter'). It was also supported by the Russian Foundation for Basic Research (Grant No. 15-02-08099) and the Scholarship Programme of the President of the Russian Federation for Young Scientists and Postgraduates Performing Promising Research and Development in High-Priority Areas of Russian Economics Modernisation (Project No. SP-703.2016.2).

## References

1. Murray J.R., Goldhar J., Eimerl D., Szoke A. *IEEE J. Quantum Electron.*, **15** (5), 342 (1979).
2. Ewing J.J., Haas R.A., Swingle J.C., George E.V., Krupke W.F. *IEEE J. Quantum Electron.*, **QE-15**, 368 (1979).
3. Jacobs R.R., Goldhar J., Eimerl D., Brown S.B., Murray J.R. *Appl. Phys. Lett.*, **37** (3), 264 (1980).

4. Gorbunov V.A., Papernyi S.B., Petrov V.F., Startsev V.R. *Sov. J. Quantum Electron*., **13** (7), 900 (1983) [*Kvantovaya Elektron*., **10** (7), 1386 (1983)].
5. Hon D.T. *Opt. Lett*., **5**, 516 (1980).
6. Maier M., Kaiser W., Giordmaine J.A. *Phys. Rev. Lett*., **17**, 1275 (1966).
7. Shilov A.A., Pasmanik G.A., Kulagin O.V. *Opt. Lett*., **26** (20), 1565 (2001).
8. Dement'ev A.S., Demin I., Murauskas E., Slavinskis S. *Quantum Electron*., **41** (2), 153 (2011) [*Kvantovaya Elektron*., **41** (2), 153 (2011)].
9. Sirazetdinov V.S., Charukhchev A.V. *Opt. Zh*., **64** (12), 85 (1997).
10. Sirazetdinov V.S., Alekseev V.N., Charukhchev A.V., Kotilev V.N., Liber V.I., Serebryakov V.A. *Proc. SPIE*, **3492**, part 2, 1002 (1999).
11. Kong H.J., Park S., Cha S., Kalal M. *Opt. Mater*., **35** (4), 807 (2013).
12. https://lasers.llnl.gov/map/index.htm.
13. Strickland D., Mourou G. *Opt. Commun*., **56** (3), 219 (1985).
14. Pennington D.M., Perry M.D., Stuart B.C., Boyd R.D., Britten J.A., Brown C.G., Herman S.M., Miller J.L., Nguyen H.T., Shore B.W., Tietbohl G.L., Yanovsky V. *Proc. SPIE*, **3047**, 490 (1997).
15. Aouama M., Yamakawa K., Akahane Y., Ma J., Inoue N., Ueda H., Kiriyama H. *Opt. Lett*., **28** (17), 1594 (2003).
16. Lozhkarev V.V., Freidman G.I., Ginzburg V.N., Katin E.V., Khazanov E.A., Kirsanov A.V., Luchinin G.A., Mal'shakov A.N., Martyanov M.A., Palashov O.V., Poteomkin A.K., Sergeev A.M., Shaykin A.A., Yakovlev I.V. *Laser Phys. Lett*., **4** (6), 421 (2007).
17. Khazanov E.A., Sergeev A.M. *Usp. Fiz. Nauk*, **178**, 1006 (2008).
18. Mak A.A., Soms L.N., Fromzel' V.A., Yashin V.E. *Lazery na neodimovom stekle* (Nd:Glass Lasers) (Moscow: Nauka, 1990).
19. Yoshida H., Kmetik V., Fujita H., Nakatsuka M., Yamanaka T., Yoshida K. *Appl. Opt*., **36** (16), 3739 (1997).
20. Kmetik V., Fiedorowicz H., Andreev A.A., Witte K.J., Daido H., Fujita H., Nakatsuka M., Yamanaka T. *Appl. Opt*., **37** (30), 7085 (1998).
21. Andreev N.F., Kulagin O.V., Palashov O.V., Pasmanik G.A., Rodchenkov V.I. *Proc. SPIE*, **2633**, 476 (1996).
22. Kafarov V.V. *Zavod. Lab*., **17** (12), 1509 (1951).
23. Kafarov V.V., Blyakhman L.I., Planovskii A.N. *Bull. Izobret. Otkrytii Tovarnykh Znakov*, (30), 141 (1974).
24. Devyatykh G.G., Rodchenkov V.I., Buevich Yu.A., Kachemtsev A.N., Sorochkin A.M., Murskii G.L. *Dokl. Akad. Nauk SSSR*, **297** (3), 661 (1987).
25. Murskii G.L., Loginov A.V., Rodchenkov V.I., Sorochkin A.M., Krylov V.A. *Vysokochist. Veshchestva*, **2** (3), 76 (1988).
26. Bespalov V.I., Pasmanik G.A. *Nelineinaya optika i adaptivnye lazernye sistemy* (Nonlinear Optics and Adaptive Laser Systems) (Moscow: Nauka, 1986).
27. Pasmanik G.A., Shklovsky E.I., Shilov A.A., in *Phase Conjugate Laser Optics.* Ed. by A. Brignon, J.-P. Huignard (Hoboken, NJ: John Wiley & Sons, Inc., 2003) p. 223.
28. Dement'ev A., Girdauskas V., Vrublevskaja O. *Nonlinear Analysis: Modelling and Control*, **7** (1), 3 (2002).